JOURNAL OF GEOPHYSICAL RESEARCH: ATMOSPHERES, VOL. 118, 8129–8139, doi:10.1002/jgrd.50602, 2013

Improved vegetation greenness increases summer atmospheric water vapor over Northern China

Bo Jiang [1,2] and Shunlin Liang [1,2,3]

Received 25 January 2013; revised 18 June 2013; accepted 24 June 2013; published 1 August 2013.

[1] Northern China is an environmentally vulnerable region with a severe water shortage. Several ecological restoration projects since the 1980s have greatly increased vegetation greenness. This study aims to assess the impacts of the changes in vegetation greenness from 1982 to 2008 on the atmospheric precipitable water (PW) over northern China during the summer seasons (June, July, and August) using reanalysis PW and satellite vegetation index data. Several statistical methods, such as linear regression (piecewise, stepwise), the Empirical Orthogonal Function, Pearson's correlation, have been used to explore the variations in and the coupling between vegetation greenness and PW. The influences of three major atmospheric circulations (the East Asian summer monsoon, the South Asian summer monsoon, and the Westerly circulation) have also been considered and excluded. The results show that summer vegetation greenness within the semi-arid western part of northern China, including the Tibetan Plateau, is closely linked to summer PW after excluding the influences of atmospheric circulations and that vegetation accounts for as much as 30% of the total PW variance. Vegetation greenness in the central and western water-limited regions of northern China has significant (>90% confidence level) positive impacts on summer PW. After investigating the relationships among evapotranspiration (ET), PW, and precipitation, it was concluded that strengthened ET driven by increased vegetation greenness makes a major contribution to increased PW. Different from the earlier hypothesis in the literature "only intact contiguous cover of natural forest having extensive borders with larger water bodies is able to keep land moisten up to an optimal for life level everywhere on land," this study found that interior forest covered regions with adequate water supply can also provide an ET benefit of PW for other regions. This study demonstrates the implications of large-scale ecological restoration projects on the hydrological cycle in arid/semi-arid regions.

Citation: Jiang, B., and S. Liang (2013), Improved vegetation greenness increases summer atmospheric water vapor over Northern China, *J. Geophys. Res. Atmos.*, *118*, 8129–8139, doi:10.1002/jgrd.50602.

1. Introduction

[2] Changes in vegetation greenness have been recognized as modifying the climate and the energy budget of the earth through both biophysical and biochemical processes [*Bonan*, 2008; *Levis*, 2010]. However, the role of vegetation in influencing hydro-climate is very controversial, and debates on this topic are usually divided into "demand-side" and "supply-side" schools [*Ellison et al.*, 2012]. The "demand-side" school suggests that an increase in vegetation could consume water and reduce runoff, which would lead to a water availability decline, especially in small-scale regions, while the "supply-side" school argues that the overall impacts of vegetation, particularly forests, are positive for water supply. For example, *Makarieva and Gorshkov* [2007, 2010] hypothesized that a "biotic pump" mechanism in continuous extensive natural forests far from coasts but having extensive borders with larger water bodies may exist. They argued that those forest covers, though far from oceans, could attract and pump moisture back into the atmosphere in the form of evapotranspiration (ET), and then, the rate at which moisture is recirculated in the form of ET may in turn have an impact on the frequency and duration of precipitation events. Although different perspectives exist, it is thought that vegetation greenness is inextricably linked to atmospheric water vapor. Until now, most studies have emphasized the role of the "biotic pumps" of interior forests from the coastal regions in altering moisture transportation and even atmospheric

[1]State Key Laboratory of Remote Sensing Science, Beijing Normal University and Institute of Remote Sensing Applications, CAS, Beijing, China.
[2]College of Global Change and Earth System Science, Beijing Normal University, Beijing, China.
[3]Department of Geographical Sciences, University of Maryland, College Park, Maryland, USA.

Corresponding author: B. Jiang, College of Global Change and Earth System Science, Beijing Normal University, Beijing 100875, China. (bojiang@bnu.edu.cn)

2169-897X/13/10.1002/jgrd.50602

circulation, and several observations have been cited to support this claim [*Angelini et al*., 2011; *Makarieva et al*., 2013; *Makarieva et al*., 2009; *Spracklen et al*., 2012; *Viste and Sorteberg*, 2013; *Sheil and Murdiyarso*, 2009; *Makarieva et al*., 2013]. However, the number of studies exploring the effects of vegetation on changes in atmospheric water shortage (e.g., precipitable water, or PW) is small [*McGuire et al*., 2006]. Although some modeling studies have recently indicated that the climatic effect of changes in long-wave radiation flux brought about by additional water vapor through ET, due to increased vegetation in middle-high northern latitudes, cannot be neglected, particularly in water-limited regions [*Rotenberg and Yakir*, 2010; *Swann et al*., 2009; *Swann et al*., 2012], direct evidence has still not been obtained.

[3] Water vapor plays a major role as a dominant feedback variable in the hydrological cycle and in radiative forcing, which impacts both global and local weather as well as climate. Water vapor in the lower troposphere not only acts as the main resource for precipitation in all weather processes by providing latent heating [*Trenberth et al*., 2005], but also influences the planetary radiative balance through cloud formation. Moreover, as a natural, important, and abundant greenhouse gas, water vapor helps maintain the Earth's surface temperature by absorbing and emitting long-wave infrared radiation, which exerts a positive feedback on the changing climate system and strengthens the greenhouse effect [*Sudradjat et al*., 2005]. Therefore, it is important to seek evidence of the impact of vegetation on PW by analyzing various data.

[4] China is located within the Asian monsoon region, meaning that its moisture content and transportation are essentially controlled by monsoon circulations. During the summer (June, July, and August (JJA)), the Asian summer monsoons (east/south) bring abundant moisture to most of mainland China and influence its precipitation pattern [*Simmonds et al*., 1999]. The moisture pattern in northern China, particularly in the arid/semi-arid parts of northwestern China, is also impacted by the westerly belt as well as by the ecosystem [*Sato et al*., 2007; *Song and Zhang*, 2003; *Wu et al*., 2012]. *Li et al*. [2009b] and *Zheng et al*. [2011] have noted that more attention needs to be paid to the influence of the land-cover and land use changes as well as other anthropogenic activities on moisture patterns. In the last three decades, China has launched large-scale ecosystem restoration programs (e.g., the Three-North Forest Shelterbelt Program, the Grain for Green project, and the Natural Forest Conservation Program) [*Liu et al*., 2008a, 2008b; *Wang et al*., 2010], especially in its northern regions, to combat environmental deterioration. Because of these efforts, forest cover has increased dramatically from 8% in 1949 to 18.2% in 2005 [*Cao et al*., 2011]. Northern China encompasses the three geographic regions of northwestern, northern, and northeastern China. These regions are severely short of water, especially the northwest. Annual precipitation is less than 400 mm over most of this region, even less than 200 mm in the northwest and therefore northern China is usually defined as a water-limited region. Because of the water shortages, the climatic effects of changes in vegetation greenness in this region have attracted worldwide attention. Previous studies of the impact of vegetation greenness change on climate in China have ranged from modeling [*Bi et al*., 2009; *Liu et al*., 2008a, 2008b; *Yu et al*., 2009; *Zheng et al*., 2002] to observational analysis [*Duan et al*., 2011; *Wu et al*., 2011; *Yang et al*., 2010], but few have explored changes in water vapor in relation to the vegetation greenness change. *Rangwala et al*. [2009] found that warming in the Tibetan Plateau has possibly been influenced by increases in water vapor, but the contributions of vegetation greenness change were not explored in their study.

[5] This study aims to investigate whether water vapor has been significantly influenced by vegetation greenness changes in the summer (JJA) over northern China and to explore the possible physical mechanisms. Details of the data sets used in this study and the analytical approach selected are provided in section 2. Section 3 describes the observed variations in water vapor in China, explores the relationship between water vapor and vegetation greenness, and discusses possible physical mechanisms for this relationship. Section 4 provides concluding remarks.

2. Methodology

2.1. Data and Study Region

[6] Vegetation greenness can be characterized using the normalized difference vegetation index (NDVI) from satellite data [*Liang et al*., 2012]. This research used the monthly, 8 km Global Inventory Monitoring and Modeling Studies NDVI products from 1982 to 2008, which are derived from data of the Advanced High Resolution Radiometer on the National Oceanic and Atmospheric Administration polar-orbiting satellite [*Tucker et al*., 2005]. This data set has been widely used for research purposes. Monthly ET satellite products from 1983 to 2006 can be obtained from *Zhang et al*. [2010]. Meteorological precipitation monthly gridded products from 1982 to 2008 can be obtained from the Climatic Research Unit [*Mitchell and Jones*, 2005].

[7] Three PW data sets were validated to determine which worked best over China. These data sets included the NASA Modern Era Retrospective-Analysis for Research and Applications (MERRA) [*Rienecker et al*., 2011], the NCEP Climate Forest System Reanalysis (NCEP/CFSR; [*Saha et al*., 2010]), and the European Center for Medium-Range Weather Forecasts Interim Reanalysis (ERA-Interim; [*Dee et al*., 2011]) with processed radiosonde station measurements by *Dai et al*. [2010] within China, station by station. The results are shown in Figure 1, which illustrates that in the summer in China, the accuracy of PW from MERRA was the most satisfactory. Therefore, the MERRA PW data set was selected for analysis in this research. All grid data sets have been aggregated into $0.5° \times 0.5°$, monthly data sets, and nonvegetated grids have been excluded [*Ma and Frank*, 2006].

[8] The 14 northern provinces in China were selected to represent northern China, as indicated in Figure 2. This area is considered to be one of the most environmentally vulnerable regions in China [*Huang et al*., 2011] and is characterized by a dry climate, severe water shortages, and land degradation. The last consists primarily of desertification caused by wind erosion, especially in the northern and

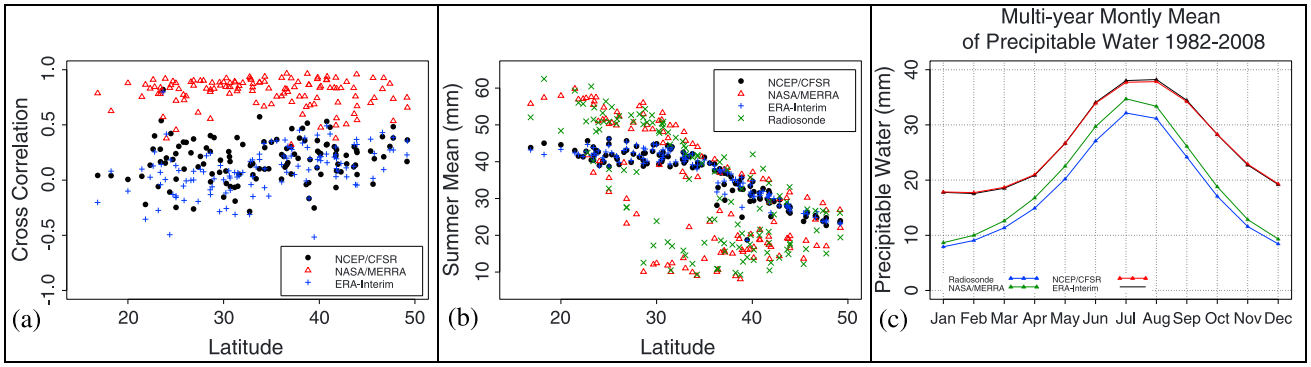

Figure 1. Validation results for three PW re-analysis products (NCEP/CFSR, NASA/MERRA, and ERA-Interim) and processed radiosonde measurements by *Dai* [2010] from 1982 to 2008. (a) Correlations between JJA re-analysis PW and measurements as a function of latitude are presented as percentages. (b) Mean values of JJA in mm of the four data sets are presented as a function of latitude. (c) Multiyear monthly means from 1982 to 2008 of the four data sets are given.

northwestern parts. Except for the northeastern region, the major types of vegetation in this area are grasses and shrubs.

2.2. Circulation Indices

[9] Most of the moisture over China is controlled by atmospheric circulations. The Asian summer monsoon (east/south) and the northern mid-high latitude westerly circulation are the main sources of moisture [*Zhang et al*., 2007]. Therefore, the three atmospheric circulation indices used in this study include the East Asian Summer Monsoon Index (EASMI), the South Asian Summer Monsoon Index (SASMI), and the Westerly Index (WI). The EASMI is a shear vorticity index, which is defined by U850 averaged in (22.5°N–32.5°N, 110°E–140°E) minus U850 in (5°N–15°N, 90°E–130°E), where U850 is the zonal wind averaged over the summer season (June-August) at 850 hPa. This index is the *Wang and Fan* [1999] index with a reverse sign and was recommended by *Wang et al*. [2008]. The SASMI is an improved index developed by *Shi et al*. [2005] based on the Webster and Yang index [*Webster and Yang*, 1992]. The improved SASMI is the optimal linear combination of the zonal wind shear U850 averaged in (7.5°N–20°N, 37.5°E–90°E) and U200 averaged in (5°N–35°N, 40°E–90°E), expressed as (2.4U850–U200), where U850 and U200 denote the zonal wind average over the season (June-September) at 850 hPa and 200 hPa, respectively. WI is an index which measures the strength of the midlatitude westerly circulation and was developed by *Rossby* [1939]. Here WI was calculated as $H_{35^\circ N} - H_{55^\circ N}$ [*Wu et al*., 2012], where H denotes the zonal-average height at 500 hPa. According to *Li et al*. [2008] and *Yan et al*. [2007], three regions were selected for calculating the regional summer (June-August) $WI_{i\ (i=1,2,3)}$ (region1: 30°E–70°E; region2: 70°E–110°E; region3:110°E–140°E), which have a close relationship with the hydro-climate within China. All the indices were generated using the MERRA reanalysis data for consistency.

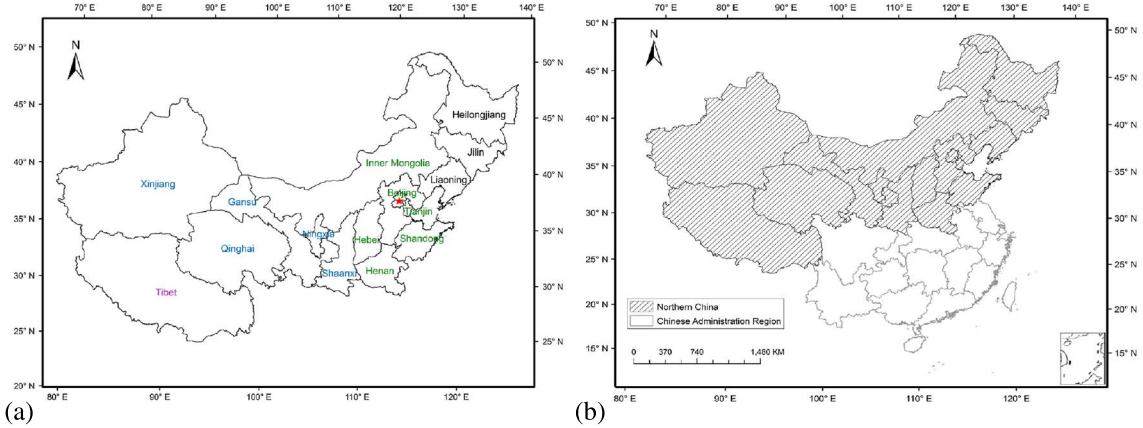

Figure 2. (a) Northern China consists of 14 provinces (from east to west): Heilongjiang, Jilin, Liaoning, Inner Mongolia Autonomous Region, Hebei, Shandong, Shanxi, Henan, Shaanxi, Ningxia Hui Autonomous Region, Gansu, Qinghai, Xinjiang Uygur Autonomous Region, and Tibet Autonomous Region. The different font color of the province name stands for the parts which this province belongs to: black means Northeastern part, green means Northern part, and blue means Northwestern part. (b) Location of Northern China over the Chinese mainland (shaded area).

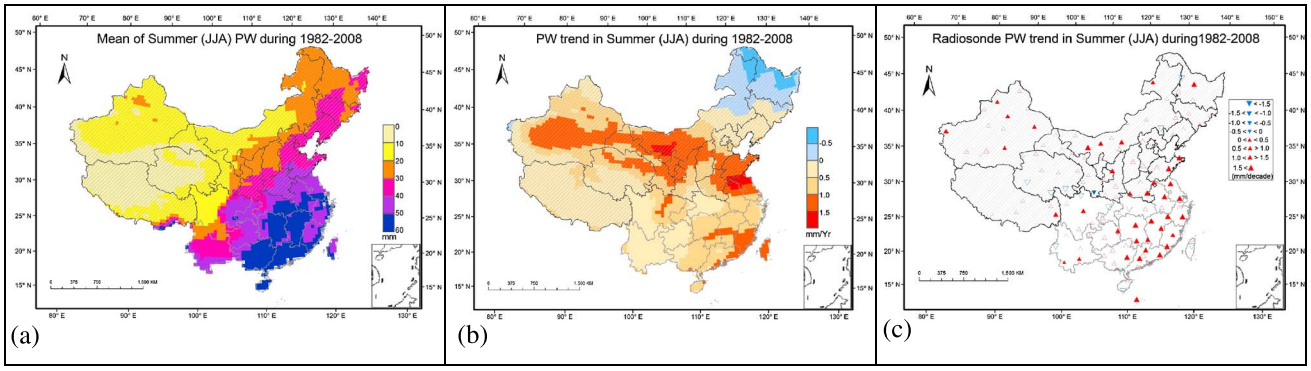

Figure 3. (a) Geographical distribution of the 27 year (1982–2008) mean summer NDVI over the Chinese mainland; (b) Geographical distribution of the mean trend of summer PW over the Chinese mainland from 1982 to 2008. (c) Geographical distribution of the trend of summer radiosonde PW measurements over the Chinese mainland from 1982 to 2008. Northern China is delineated by a black line.

2.3. Statistical Methods

[10] Several statistical methods were used to investigate the spatiotemporal variation of the variables and their linkages in the summer from 1982 to 2008. Because the PW has a very short memory, only the simultaneous effects of variables were considered in the following analysis.

[11] The analysis proceeded in four steps. First, linear regression was carried out to analyze trends in summer NDVI and PW over China during this period. Second, an Empirical Orthogonal Function (EOF) analysis was conducted for summer PW anomalies. The EOF method is thought to be one of the most effective ways to explore the spatiotemporal structure of the long-term variations of a variable over a specific area and is based on the covariance matrix. The summer PW anomalies were derived by removing the annual cycle (subtracting long-term mean values) from all grid point time series. Third, Pearson's correlation was used to explore coupling between variables. To determine whether there is a persistent trend in the summer for northern China's PW and NDVI activity, a piecewise linear regression model [*Toms and Lesperance*, 2003] was used to detect their turning points (TPs) in the fourth step. The model used is:

$$y = \begin{cases} \beta_0 + \beta_1 t + \varepsilon & (t \le \alpha) \\ \beta_0 + \beta_1 t + \beta_2 (t - \alpha) + \varepsilon & (t > \alpha) \end{cases} \quad (1)$$

where t is the year, y is summer (JJA) PW or NDVI, α is the TP of the summer PW or NDVI trend, β_0, β_1, and β_2 are regression coefficients, and ε is the residual of the fit. The summer linear PW or NDVI trend is β_1 before the TP and $\beta_1 + \beta_2$ after it. α was determined by the least squares error method. TP was confined to the period from 1986 to 2002 to avoid linear regression in one period with too few data points, and the significance of TP was tested using a t test. A p value <0.1 was considered significant. For more details, the readers can refer to *Wang et al.* [2011].

[12] These methods cannot quantify the effect of NDVI on PW. To explore further how terrestrial vegetation changes have impacted PW, it is necessary to consider the impacts of atmospheric circulations and the TP of PW together. Based on this assertion and the assumption that the relationship is linear, two scenarios were represented: The first takes into account only the influence of the circulations and can be written as:

$$PW = a + bYear + c(Year - \alpha) + d_m \sum_{m=1}^{5} X_m + \varepsilon, \quad (2)$$

where ε represents the residuals (or errors) of the regression; a, b, c, and d_m are regression coefficients, which are estimated pixel by pixel by the ordinary least squares (OLS) method; $X_{m(m=1,2,\ldots,5)}$ contains the circulation indices EASMI, SASMI, and $WI_{i=1,2,3}$, and optimal stepwise linear regression is used to select the most relevant circulation indices based on the Akaike Information Criterion. The variables "year" and "α" are included in equation (2) to account for a possible trend and TP in the PW. This equation states that year-to-year changes in PW during the summer are linearly related to year-to-year changes in the atmospheric circulations. The second scenario incorporates the same variables and the observed summer NDVI together:

$$PW = a' + b'Year + c'(Year - \alpha) + d'_m \sum_{m=1}^{5} X_m + eNDVI + \varepsilon'. \quad (3)$$

[13] This interactive scenario clarifies the influence of NDVI on PW, in which X_m are the optimal selected circulation indices from equation (2), and all the coefficients were also estimated by the OLS. Finally, *F-test* was conducted to determine the statistical significance of the coefficient e in equation (3), which indicates to what extent a relation exists. The nature of this effect is indicated by the sign of e; a positive value indicates that increases in NDVI increases PW.

3. Results and Analysis

[14] The analytical results of the spatiotemporal variations and coupling between summer PW and NDVI in the study region are presented in this section. The effect of NDVI on PW has also been quantified. As a deeper analysis, the relations

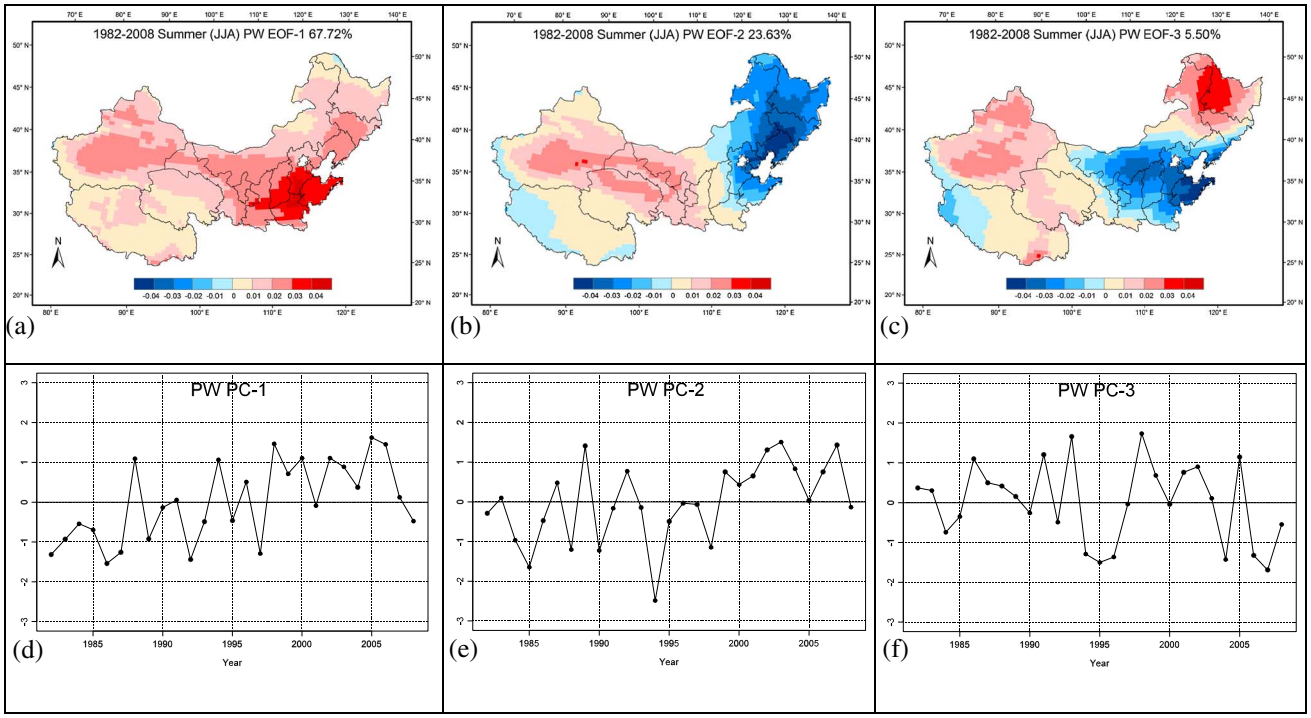

Figure 4. (a, b, and c) First three leading eigenvectors and (d, e, and f) associated principal components obtained from EOF analysis of summer mean PW anomalies over northern China from 1982 to 2008. Colors represent positive and negative values.

between ET, PW, and P are also explored to help clarify the physical mechanisms involved.

3.1. Changes in Summer PW

[15] The first step was to examine the geographical distribution of the mean and the linear trend of summer PW based on the MERRA reanalysis data from 1982 to 2008 at the national scale, as shown in Figure 3. The spatial distribution of the summer PW means in Figure 3a indicates an obvious decreasing trend from east to west in China. The Tibet Autonomous Region, Qinghai, Gansu, and the southern Xinjiang Uygur Autonomous region desert areas within western China show PW values less than 10 mm, while other eastern regions, which are mostly influenced by the Asian monsoon, have relatively abundant water vapor. Figure 3b shows the spatial pattern of summer PW trends during the same period with an average rate of 0.057 mm yr^{-1}. This means a general increasing trend in PW in most of China, and in several areas located in western China, such as the central Inner Mongolia Autonomous Region, the Ningxia Hui Autonomous Region, Gansu Province, and the Xinjiang Uygur Autonomous Region. To prove the reliability of the MERRA PW products further, the results for the linear trend of PW radiosonde measurements are also shown in Figure 3c, which show a generally similar pattern to Figure 3b. In other words, the dry arid/semi-arid regions within northern China (delineated by the black line in Figure 3) have been becoming moister in the last three decades.

[16] In addition to the 27 year climatology and summer PW trend, an examination of the spatiotemporal pattern of PW changes over the whole of northern China is interesting. An EOF analysis was conducted of the anomalies in summer PW from 1982 to 2008. Figure 4 shows the first three leading modes of PW, which together explain 96.85% of the total variance. The first mode accounts for 67.72% of the variance; its spatial pattern (Figure 4a) is generally characterized by a same positive sign over the whole study region, while its corresponding Principal Component (PC) time series (Figure 4d) shows a generally increasing trend throughout the analysis period. This indicates that summer PW over northern China is most likely increasing. According to *Zhai and Eskridge* [1997] and *Xie et al.* [2011], this trend is strongly coupled with an increasing trend in surface temperature in the warm season. Moreover, there appears to be an increasing trend until 2000 and a relatively stable situation afterwards. The second mode (Figure 4b), which explains 23.63% of the variance, seems to separate the signal into a west-east pattern. It is characterized by positive anomalies in the northern and northwestern arid/semi-arid regions west of 110°E and negative anomalies in northeastern part of China and the southeastern and southwestern Tibet Autonomous Region. The associated PC time series in Figure 4e shows a sudden increasing trend after the mid to late1990s, reflecting an apparent strengthening in PW over the western arid/semi-arid regions and a steady decrease in northeastern China since the mid-1990s. Although the third mode of PW (Figure 4c) explains 5.50% of the variance, it indicates subregional dipole-like PW changes from west to east. The corresponding time series (Figure 4f) shows an interannual variation and also a TP around the mid-1990s. The three modes together reflect different patterns of PW variation in the western and eastern parts of northern China, as well as a change in summer PW patterns which has been occurring since the mid-1990s or the beginning of the 2000s.

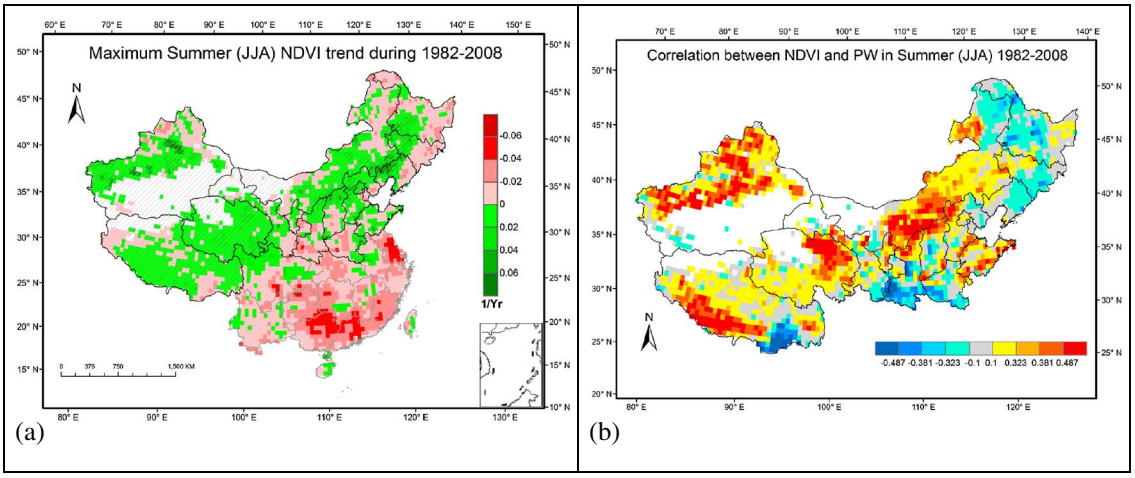

Figure 5. (a) Linear regression trends in maximum summer (JJA) NDVI over the Chinese mainland from 1982 to 2008; (b) Pearson's correlation results between summer NDVI and PW over northern China from 1982 to 2008. Northern China is delineated by the black line.

[17] These findings mostly agree with *Xie et al*. [2011]. However, the results of this research indicate that northeastern China has experienced a decreasing trend in summer PW, especially after the mid-1990s, which is in disagreement with previous work [*Xie et al*., 2011; *Zhai and Eskridge*, 1997] due to the different periods considered. The northeastern region of China is mainly located north of 40°N and east of 115°E, and its moisture is controlled mostly by the East Asian summer monsoon. According to *Zou et al*. [2005] and *Piao et al*. [2010], the observations could be explained by the decreased EASM, warming, and droughts in recent decades. Besides, several studies did show a decline in moisture over the Tibet Autonomous Region [*Xie et al*., 2011; *Wang and Guo*, 2011], but this was not always found to be the case in the present research, whether using reanalysis data or radiosonde measurements (Figures 3b and 3c), and it is still unclear how this phenomenon is related to changes in surface vegetation. Therefore, PW variation is most likely different from west to east within northern China because of natural conditions. In addition, PW is notably more influenced by other factors in the western arid/semi-arid regions of northern China.

3.2. PW Links to Changes in NDVI Over Northern China

[18] To examine the links between PW and NDVI over northern China, the linear trend of maximum summer NDVI at the national scale from 1982 to 2008, as shown in Figure 5a, was examined. It shows strong spatial heterogeneity, but the great contrast between northern China (delineated by the black line) and southern China is very clear. Most of central and southern China showed a decreasing trend in summer NDVI, while northern China and most of its northwestern part had an increased NDVI from 1982 to 2008. Overall, an increased NDVI was found in 40.30% (90% significant increase in 18.45% of the pixels) of China's land area in the summer. This result is also consistent with those reported by *Peng et al*. [2011]. Both Figures 3b and 5a indicate that most regions of northern China, mainly in its central and western part, became greener and moister in summer from 1982 to 2008. Furthermore, a linear Pearson's correlation result between summer NDVI and PW over northern China from 1982 to 2008 is shown in Figure 5b. This result presents a positive relation, mostly in the western and central Inner Mongolia Autonomous Region, which suggests that increased PW in these regions can possibly be attributed to increased summer NDVI.

[19] Although Figure 5b reveals a strong link between NDVI and PW in the study region, it does not take the TPs of the two variables into account. However, previous studies have explored and identified the TPs of vegetation changes. For example, *Park and Sohn* [2010] noted that a TP in vegetation variation observed in the mid-1990s existed in mid-high latitudes over the northern hemisphere from 1982 to 2006, and *Peng et al*. [2011] found that the change occurred around the 2000s in northern China in the growing season. Meanwhile, EOF modes 2 and 3 of the PW, as described in section 3.1, also suggest that a TP appeared in the summer PW over northern China around the mid-1990s. Therefore, if a coupling between PW and NDVI does exist, the geographical distribution of the TPs in the summer trends of the two variables should be similar. To determine whether this is true, a piecewise linear regression approach was used to identify the TPs of the summer PW and NDVI trends, with the results shown in Figures 6a and 6b, respectively. The spatial distributions of the trends in summer PW and NDVI before and after the PW TPs are displayed in Figures 6c–f.

[20] The significance level of the TPs in Figures 6a and 6b are both greater than 90%. Figure 6a shows that the TPs of summer PW occurred mostly in the northern Xinjiang Uygur Autonomous Region and the central Tibet Autonomous Region around the 2000s, which is most consistent with the TP distribution of summer NDVI in these areas (red box) as shown in Figure 6b. Figures 6c and 6e show the spatial distributions of the trend in summer PW before and after its TP. Clearly opposite trends can be observed when comparing these two plots. Before the PW TP, 94.27% of the pixels with significant TPs show an increasing trend in summer PW, which suggests a more

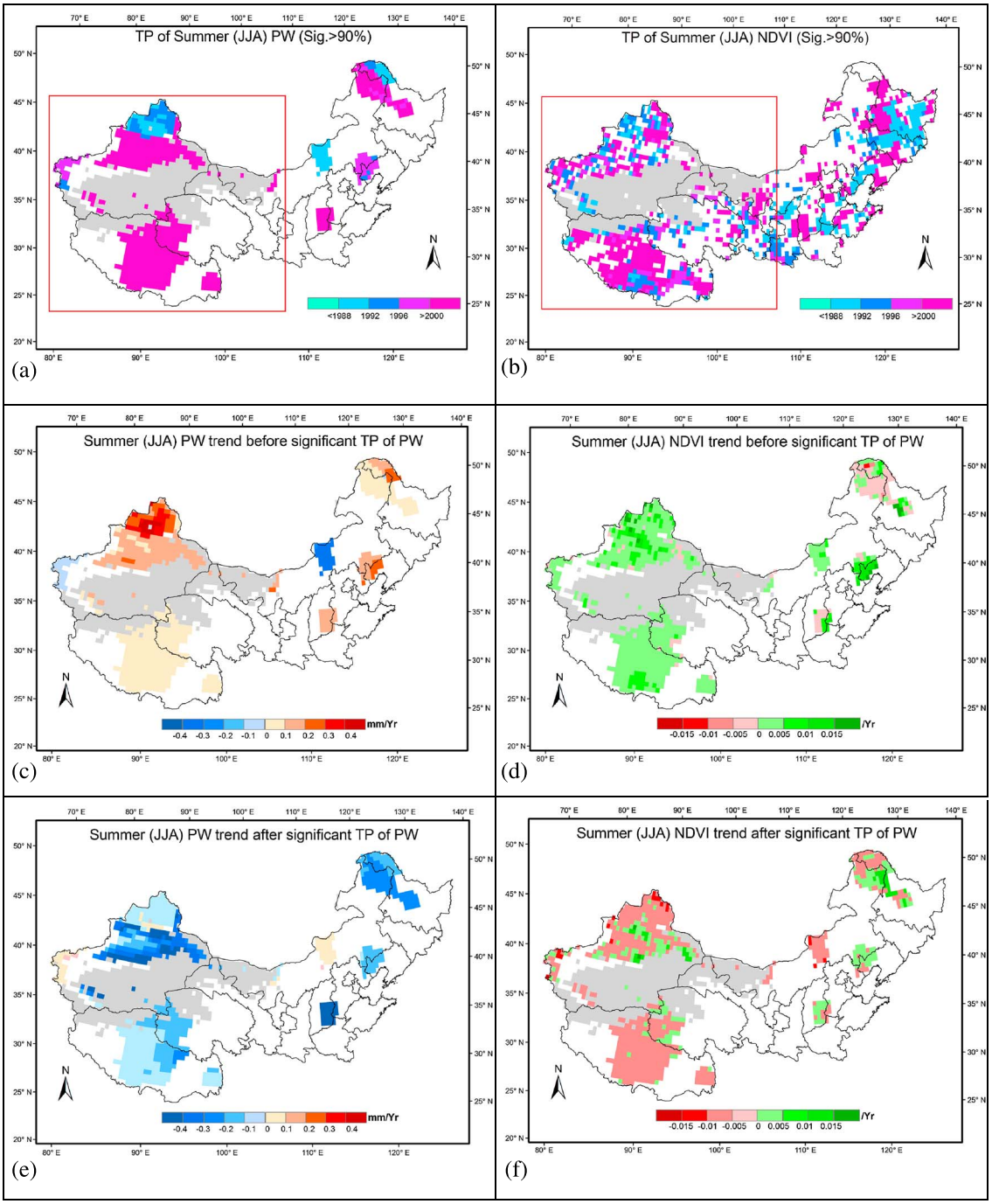

Figure 6. Spatial distribution of changes in summer (JJA) PW and NDVI over northern China analyzed using the piecewise regression approach. Turning point (TP) of (a) PW and (b) NDVI. Trends in summer PW (c) before its TP and (e) after its TP. Trends in summer NDVI (d) before the TP of summer PW and (f) after the TP of summer PW. Red boxes in Figures 6a and 6b indicate the hot spot regions: northern Xinjiang Uygur Autonomous Region and the central Tibet Autonomous Region. Gray color represents nonvegetated area. White areas indicate the pixels whose TPs are insignificant at the 90% confidence level.

humid climate in the western area over northern China. However, after the TP, the climate becomes more and more dry. At the same time, the trends in summer NDVI in these two hot spot regions (northern Xinjiang Uygur Autonomous Region and central Tibet Autonomous Region) are consistent with PW; NDVI shows similar trends to PW, which again suggests that increased (decreased) vegetation may be attributed to a wetter (drier) climate in northwestern China.

[21] Overall, the analytical results demonstrate that the central and western parts of northern China are the most sensitive region for interaction between NDVI and PW, while PW in the northeastern region is influenced more by atmospheric circulations.

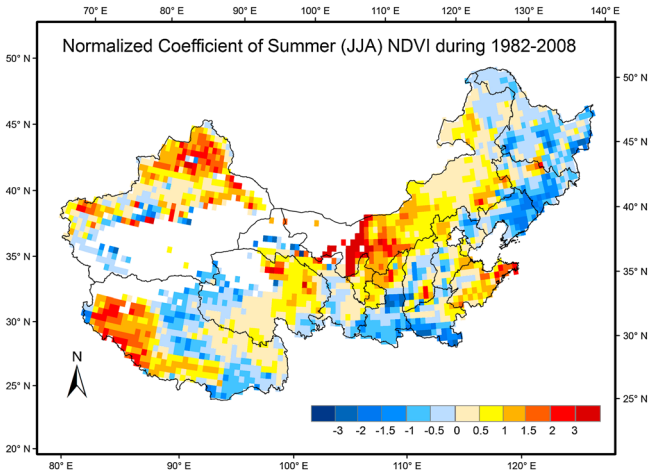

Figure 7. Coefficients *e* of NDVI in summer from 1982 to 2008 over northern China. The coefficients are normalized by their respective standard deviations.

3.3. Effects of NDVI on PW

[22] According to the analysis described above, NDVI changes are highly correlated with changes in PW in northern China in the summer, especially over the central and western arid/semi-arid regions. The actual effect of vegetation changes on regional PW cannot be assessed without excluding the influences of atmospheric circulations. The impacts of major atmospheric circulations such as EASM, SASM, and WI, as mentioned in section 2.2, are discussed below.

[23] By building two scenarios and using the optimal stepwise linear regression method, as well as taking into account the TPs of the PW, the standardized coefficient *e* in equation (3) has been estimated pixel by pixel over northern China, with result shown in Figure 7. It is obvious that *e* is positive in most regions of northern China, particularly in the central and western water-limited areas, and negative in the three provinces of northeastern China (Heilongjiang, Jilin, and Liaoning), south of the central provinces, and in the southeastern Tibet Autonomous Region. This result matches previous findings by the authors, and its pattern is similar to that shown in Figure 5b. This finding indicates that increased vegetation greenness in most northern nonmonsoon regions, as well as the Tibet Autonomous Region, is a possible reason for the observed increases in atmospheric water content, which has important implications for water cycle in this area, especially in arid/semi-arid regions.

[24] After testing the significance of the *e* values using the *F-test*, the pixels with a significance level greater than 90% were selected and are shown in Figure 8a. The corresponding variances in PW explained by the NDVI of these pixels, which are measured in terms of the difference between the square of the correlation coefficients (R^2) of the two scenarios, are shown in Figure 8b. Overall, there are four major regions where NDVI has positive influence on PW over northern China (indicated by red boxes in Figure 8a): the central part of the Inner Mongolia Autonomous Region (box 1), the northern of Xinjiang Uygur Autonomous Region (box 2), the Eastern Qinghai Province (box 3), and the southwestern Tibet Autonomous Region (box 4). Figure 8b shows that almost all the R^2 values increased in the four regions, with the largest increase being as much as 30%, indicating that summer vegetation greenness in the four regions is very closely linked to PW and accounts for as much as 30% of the total PW variance from1982 to 2008. It is very interesting to note that all these regions are mountainous: the central part of the Inner Mongolia Autonomous Region is south of the Yin Mountains, the northern Xinjiang Uygur Autonomous Region is north of the Tianshan Mountain area, the eastern part of Qinghai Province is located in the eastern Qilian Mountains, and the southwestern Tibet Autonomous Region is part of the Himalayas. Due to their special topography and geolocation, these four regions have relatively abundant available water for vegetation, even for forest. Moreover, the first

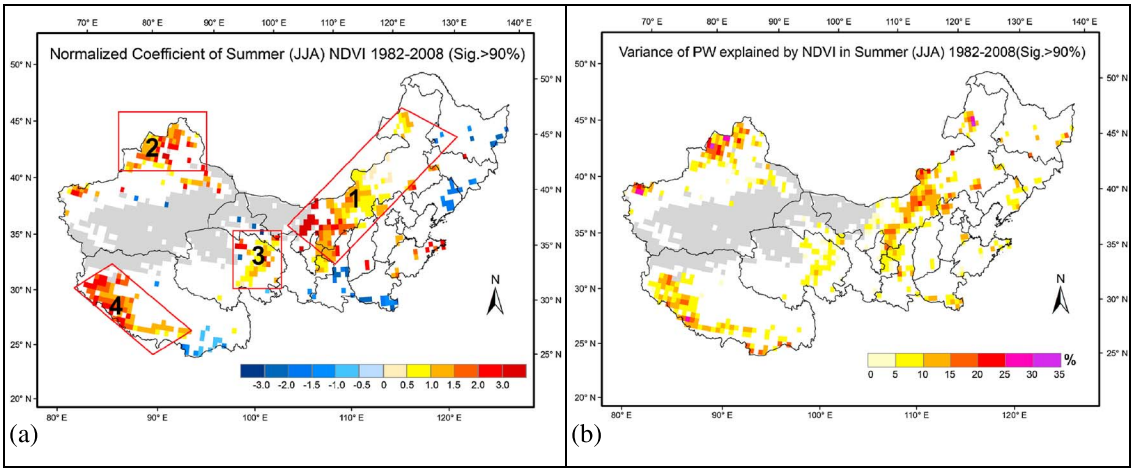

Figure 8. Significant (>90% confidence level) regions of (a) coefficient *e* of NDVI, and (b) the corresponding explained PW variance by NDVI in summer from 1982 to 2008 over northern China. The four red boxes in Figure 8a indicate the most sensitive regions for the positive influence of NDVI on PW: central Inner Mongolia Autonomous Region (1), northern Xinjiang Uygur Autonomous Region (2), western Qinghai Province (3), and southwestern Tibet Autonomous Region (4). Gray color represents nonvegetated area.

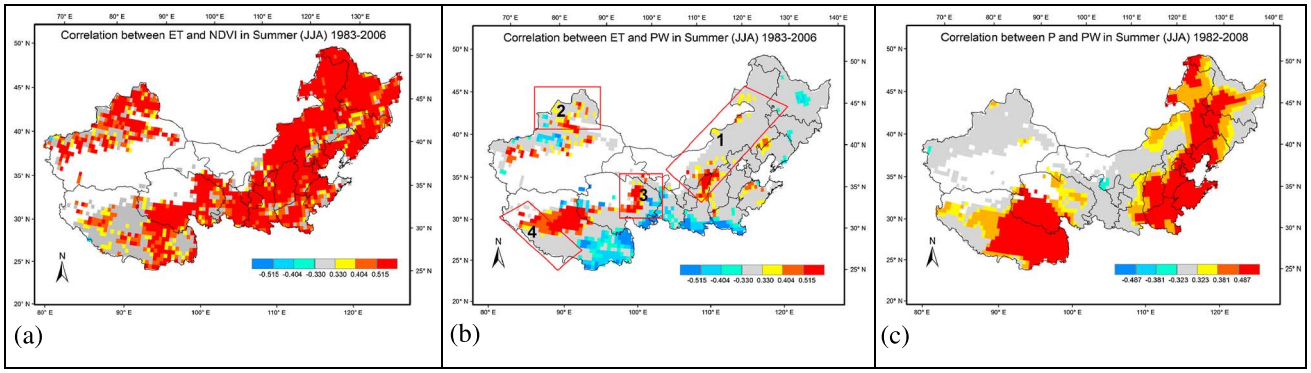

Figure 9. Correlation between (a) ET and NDVI in summer from 1983 to 2006, (b) ET and PW in summer from 1983 to 2006, and (c) precipitation (P) and PW in summer from 1982 to 2008 over northern China. The four red boxes in Figure 9b are the same as in Figure 8a. The numbers in the legend indicate the significance level: 90%, 95%, and 99%.

region (box 1) is within the ecological transitional zone, which is the most sensitive region for the vegetation-climate interaction over northern China [*Dessler et al*., 2008]. Note that summer vegetation increased markedly in these regions during the study period, as shown in Figure 5a. The significantly negatively influenced regions, by contrast, are scarce and scattered. The vegetation activity in these regions makes little contribution to the variation of local PW, except for some forest areas in southeastern Tibet Autonomous Region.

[25] The ET process is a possible physical mechanism for the positive impact of vegetation changes on PW. Vegetation transpiration transfers water vapor into the atmosphere, meaning that increased vegetation greenness may contribute to the regional availability of atmospheric moisture vapor, in particular in arid and semi-arid regions, where the hydro-climate is closely linked to local moisture recycling, which is strongly affected by local vegetation greenness [*Makarieva et al*., 2009; *Wang and Dickinson*, 2012; *Wu et al*., 2012]. Moreover, *Ellison et al*. [2012] assumed that forest-driven ET process also contributes to the atmospheric moisture vapor cross-continental transport and intensifies the regional water cycle, though *Makarieva and Gorshkov* [2007] claimed that this "biotic pump" could be created only by the intact contiguous cover of natural forest from the coastal regions. To verify their points, the correlation between summer season ET and PW over northern China was examined, with results shown in Figure 9a. Here only the period from 1983 to 2006 was analyzed because the ET data set was the only available data set. It is obvious that ET is generally positively correlated with PW, and most of the significant areas are located in the four regions shown in Figure 8a.This demonstrates that, on one hand, strengthened ET driven by increased vegetation greenness is one of the major sources for water vapor in the atmosphere, and on the other hand, the fact that ET is not strongly related to PW in some areas of the four hot spot regions (i.e., gray areas in box 1) demonstrates that increased forest cover over the four regions could help transport additional PW from regions with a surplus to other regions that lack adequate moisture availability. However, in regions where PW is controlled mostly by monsoons, such as the northeast, the effect of vegetation on PW is minor, although forest cover has increased markedly. It is also noteworthy that vegetation greenness in the southeastern Tibet Autonomous Region is negatively correlated with regional water vapor and that vegetation here decreased during the study period (Figure 5a). According to *Zhang et al*. [2011], the increased vegetation greenness in the southeastern Tibet Autonomous Region is influencing the Bowen ratio, which tends to enhance vertical ascending motion and forces more atmospheric moisture to precipitate out. *Wang et al*. [2011] also pointed out that the precipitable-water conversion rates over southeastern Tibet decreased from 1970 to 2009, which is a possible reason that PW has increased. This may explain the decreased vegetation greenness accompanied by increased atmospheric water vapor in the southeastern Tibet Autonomous region. In addition, the thermal effect, which refers mainly to the alteration of air temperature due to change in the solar energy absorption and energy partitioning into latent and sensible fluxes accompanied by changes in vegetation and water vapor, also influences the PW by altering ET process and the water-vapor holding capacity.

[26] The results shown in Figures 9a and 9b have verified our hypothesis that ET driven by increased vegetation greenness makes a major contribution to increased atmospheric water vapor in water-shortage-afflicted northwestern China. Nevertheless, the opposite hypothesis that increased PW causes increased NDVI through increased precipitation might still be proposed. It is worth noting that the precipitation that occurs barely satisfies the needs for vegetation growth in the arid/semi-arid areas of northwestern China, even in the summer season in which most precipitation occurs. If this is the case, then the spatial pattern of the correlation between precipitation and PW should be similar to that between ET and PW. Further examination reveals that the correlation between precipitation and PW (see Figure 9c) does not exhibit patterns similar to Figure 9b and the relation is especially poor for the four hot regions. This helps to demonstrate that increased vegetation greenness in the summer would increase local water vapor within the nonmonsoon-impacted, water-shortage-afflicted northwestern China region. Moreover, this conclusion is also supported by some numerical simulation studies [*Liu et al*., 2008a, 2008b].

4. Summary and Discussions

[27] Water vapor is an important greenhouse gas that accounts for 50% to 75% of the greenhouse effect today [*Ravishankara*, 2012] and is a key driver of many atmospheric processes. Although the positive trend in the summer PW over China, especially in northern China, has been documented by many previous studies [*Li et al*., 2009a; *Xie et al*., 2011; *Zhai and Eskridge*, 1997], this study has demonstrated that this trend can be largely attributed to increased vegetation greenness through ET after several ecosystem restoration projects have been implemented during the last three decades over northern China.

[28] This study began by examining the spatiotemporal variations of PW and vegetation and then established the relationship between changes in PW and vegetation changes in the summer (June-August) over northern China using seasonal mean PW and maximum NDVI data for the period from 1982 to 2008. Finally, the effect of vegetation changes on local PW were identified and quantified by excluding the influences of major atmospheric circulations.

[29] An analysis of PW and NDVI data sets confirmed the general positive trends and the strong spatiotemporal coupling variations of these two variables in the summer over most of northern China, especially in its central and western parts. After removing the influences of atmospheric circulation indices (EASMI, SASMI, WI), the increases in NDVI were found to be partly responsible for increased atmospheric water-vapor content over most parts of northern China, in particular the nonmonsoon interior water-limited regions. This finding is consistent with those of *Wu et al*. [2012] for the Tarim River Basin. Further analyses were conducted to identify the most sensitive regions for vegetation-PW interaction, and four regions where NDVI had significant positive impact on PW were identified. In these regions, NDVI can account for as much as 30% of the variance in PW.

[30] To explore how increased vegetation greenness strengthens PW in the four regions, the relation between ET and NDVI and, between ET and PW from 1983 to 2006 and the correlation between precipitation and PW from 1982 to 2008 were investigated in the four regions. All the results suggested that (1) ET controlled by terrestrial vegetation is one of the major sources of regional atmospheric water vapor in interior regions far from oceans, and (2) in mountainous areas, mainly covered by forest due to the adequate water supply, the local moisture cycle is intensified and reinforced because of the ecological functions of forest besides ET.

[31] Based on this evidence, it can be concluded that vegetation is very important to the moisture cycle in arid/semi-arid regions over northern China. In regions where water is amply sufficient for vegetation, the presence of forest can have more influence on moisture cycling. These findings have great implications for assessments of the greenhouse effect and water-resources management in water-limited regions.

[32] However, other factors, such as changes in glacial extent, irrigation, and drought over northern China, need to be further explored. The nonlinear relation between vegetation and PW also needs to be explored in a subsequent study.

[33] **Acknowledgments.** The authors would like to thank Aiguo Dai for providing the homogenized daily radiosonde precipitable water data. They would also like to thank the anonymous reviewers for their valuable suggestions and comments.

References

Angelini, I., M. Garstang, R. Davis, B. Hayden, D. Fitzjarrald, D. Legates, S. Greco, S. Macko, and V. Connors (2011), On the coupling between vegetation and the atmosphere, *Theor. Appl. Climatol.*, *105*(1), 243–261.

Bi, H. X., B. Liu, J. Wu, L. Yun, Z. H. Chen, and Z. W. Cui (2009), Effects of precipitation and landuse on runoff during the past 50 years in a typical watershed in the Loess Plateau, China, *Int. J. Sediment Res.*, *24*(3), 352–364.

Bonan, G. B. (2008), Forests and climate change: Forcings, feedbacks, and the climate benefits of forests, *Science*, *320*(5882), 1,444–1,449.

Cao, S., L. Chen, D. Shankman, C. Wang, X. Wang, and H. Zhang (2011), Excessive reliance on afforestation in China's arid and semi-arid regions: Lessons in ecological restoration, *Earth Sci. Rev.*, *104*(4), 240–245.

Dai, A., J. Wang, P. W. Thorne, D. E. Parker, L. Haimberger, and X. L. Wang (2010), A new approach to homogenize daily radiosonde humidity data, *J. Climate*, *24*(4), 965–991.

Dee, D. P., et al. (2011), The ERA-Interim reanalysis: Configuration and performance of the data assimilation system, *Q. J. R. Meteorol. Soc.*, *137*(656), 553–597.

Dessler, A. E., P. Yang, J. Lee, J. Solbrig, Z. Zhang, and K. Minschwaner (2008), An analysis of the dependence of clear-sky top-of-atmosphere outgoing longwave radiation on atmospheric temperature and water vapor, *J. Geophys. Res.*, *113*, D17102, doi:10.1029/2008JD010137.

Duan, H., C. Yan, A. Tsunekawa, X. Song, S. Li, and J. Xie (2011), Assessing vegetation dynamics in the Three-North Shelter Forest region of China using AVHRR NDVI data. *Environmental Earth Sciences*, *64*(4), 1011–1020.

Ellison, D., M. N. Futter, and K. Bishop (2012), On the forest cover–water yield debate: From demand- to supply-side thinking, *Glob. Change Biol.*, *18*(3), 806–820.

Huang, G., Y. Liu, and R. Huang (2011), The interannual variability of summer rainfall in the arid and semiarid regions of Northern China and its association with the northern hemisphere circumglobal teleconnection, *Adv. Atmos. Sci.*, *28*(2), 257–268.

Levis, S. (2010), Modeling vegetation and land use in models of the Earth System, *Wiley Interdiscip. Rev. Clim. Change*, *1*(6), 17.

Li, W. L., K. L. Wang, S. M. Fu, and H. Jiang (2008), The interrelationship between regional westerly index and water vapor budget in Northwest China, *J. Glaciology and Geocryology*, *30*(1), 28–34.

Li, J. B., E. R. Cook, R. D'Arrigo, F. H. Chen, and X. H. Gou (2009a), Moisture variability across China and Mongolia: 1951–2005, *Climate Dynam.*, *32*(7–8), 1,173–1,186.

Li, J. B., et al. (2009b), Summer monsoon moisture variability over China and Mongolia during the past four centuries, *Geophys. Res. Lett.*, *36*, L22705, doi:10.1029/2009GL041162.

Liang, S., X. Li, and J. Wang (editors), (2012), *Advanced Remote Sensing: Terrestrial Information Extraction and Applications*, Academic Press, Beijing.

Liu, J. G., S. X. Li, Z. Y. Ouyang, C. Tam, and X. D. Chen (2008a), Ecological and socioeconomic effects of China's policies for ecosystem services, *Proc. Natl. Acad. Sci. U. S. A.*, *105*(28), 9,477–9,482.

Liu, Y., J. Stanturf, and H. Lu (2008b), Modeling the potential of the Northern China forest shelterbelt in improving hydroclimate conditions, *J. Am. Water Resour. Assoc.*, *44*(5), 1,176–1,192.

Ma, M., and V. Frank (2006), Interannual variability of vegetation cover in the Chinese Heihe River Basin and its relation to meteorological parameters, *Int. J. Remote Sens.*, *27*(16), 3,473–3,486.

Makarieva, A., and V. Gorshkov (2007), Biotic pump of atmospheric moisture as driver of the hydrological cycle on land, *Hydrol. Earth Syst. Sci. Discussions*, *11*(2), 1,013–1,033.

Makarieva, A. M., and V. G. Gorshkov (2010), The Biotic Pump: Condensation, atmospheric dynamics and climate, *Int. J. Water*, *5*(4), 365–385.

Makarieva, A. M., V. G. Gorshkov, and B.-L. Li (2009), Precipitation on land versus distance from the ocean: Evidence for a forest pump of atmospheric moisture, *Ecol. Complex.*, *6*(3), 302–307.

Makarieva, A., V. Gorshkov, and B.-L. Li (2012), Revisiting forest impact on atmospheric water vapor transport and precipitation, *Theor. Appl. Climatol.*, *1–18*.

Makarieva, A., V. Gorshkov, et al. (2013), Where do winds come from? A new theory on how water vapor condensation influences atmospheric pressure and dynamics, *Atmos. Chem. Phys*, *13*, 1,039–1,056.

McGuire, A. D., F. S. Chapin, J. E. Walsh, and C. Wirth (2006), Integrated regional changes in arctic climate feedbacks: Implications for the global climate system, in *Annual Review of Environment and Resources*, edited, Annual Reviews, Palo Alto, pp. 61–91 .

Mitchell, T. D., and P. D. Jones (2005), An improved method of constructing a database of monthly climate observations and associated high-resolution grids, *Int. J. Climatol.*, *25*(6), 693–712.

Park, H. S., and B. J. Sohn (2010), Recent trends in changes of vegetation over East Asia coupled with temperature and rainfall variations, *J. Geophys. Res.*, *115*, 12, D14101, doi:10.1029/2009JD012752.

Peng, S. S., A. P. Chen, L. Xu, C. X. Cao, J. Y. Fang, B. M. Ranga, E. P. Jorge, J. T. Compton, and S. L. Piao (2011), Recent change of vegetation growth trend in China, *Environ. Res. Lett.*, *6*(4), 044,027.

Piao, S. et al. (2010), The impacts of climate change on water resources and agriculture in China, *Nature*, *467*(7311), 43–51.

Rangwala, I., J. R. Miller, and M. Xu (2009), Warming in the Tibetan Plateau: Possible influences of the changes in surface water vapor, *Geophys. Res. Lett.*, *36*, L06703, doi:10.1029/2009GL037245.

Ravishankara, A. R. (2012), Water vapor in the lower stratosphere, *Science*, *337*(6096), 809–810.

Rienecker, M. M., et al. (2011), MERRA: NASA's Modern-Era Retrospective Analysis for Research and Applications, *J. Climate*, *24*(14), 3,624–3,648.

Rossby, C. G. (1939), Relation between variations in the intensity of the zonal circulation of the atmosphere and the displacements of the semi-permanent centers of action, *J. Mar. Res.*, *2*(1), 38–55.

Rotenberg, E., and D. Yakir (2010), Contribution of semi-arid forests to the climate system, *Science*, *327*(5964), 451–454.

Saha, S., et al. (2010), The NCEP Climate Forecast System Reanalysis, *Bull. Am. Meteorol. Soc.*, *91*(8), 1,015–1,057.

Sato, T., M. Tsujimura, T. Yamanaka, H. Iwasaki, A. Sugimoto, M. Sugita, F. Kimura, G. Davaa, and D. Oyunbaatar (2007), Water sources in semi-arid northeast Asia as revealed by field observations and isotope transport model, *J. Geophys. Res.*, *112*, D17112, doi:10.1029/2006JD008321.

Sheil, D., and D. Murdiyarso (2009). How forests attract rain: An examination of a new hypothesis, *Bioscience*, *59*(4), 341–347.

Shi, N., J. Q. Gu, Y. M. Yi, and Z. M. Lin (2005), An improved south Asian summer monsoon index with Monte Carlo test, *Chin. Phys.*, *14*(4), 844–849.

Simmonds, I., D. H. Bi, and P. Hope (1999), Atmospheric water vapor flux and its association with rainfall over China in summer, *J. Climate*, *12*(5), 1,353–1,367.

Song, L. C., and C. J. Zhang (2003), Variable character of precipitation in Northwest China in recent 20 century, *J. Glaciology and Geo-cryology*, *25*(2), 143–148.

Spracklen, D. V., S. R. Arnold, and C. M. Taylor (2012), Observations of increased tropical rainfall preceded by air passage over forests, *Nature*, *489*(7415), 282–285.

Sudradjat, A., R. R. Ferraro, and M. Fiorino (2005), A comparison of total precipitable water between reanalyses and NVAP, *J. Climate*, *18*(11), 1,790–1,807.

Swann, A., I. Fung, S. Levis, G. Bonan, and S. Doney (2009), Changes in Arctic vegetation amplify high-latitude warming through the greenhouse effect, *Proc. Natl. Acad. Sci.*, *107*(4), 1,295–1,300.

Swann, A. L. S., I. Y. Fung, and J. C. H. Chiang (2012), Mid-latitude afforestation shifts general circulation and tropical precipitation, *Proc. Natl. Acad. Sci.*, *109*(3), 712–716.

Toms, J. D., and M. L. Lesperance (2003), Piecewise regression: A tool for identifying ecological thresholds, *Ecology*, *84*(8), 2,034–2,041.

Trenberth, K., J. Fasullo, and L. Smith (2005), Trends and variability in column-integrated atmospheric water vapor, *Climate Dynam.*, *24*(7), 741–758.

Tucker, C. J., J. E. Pinzon, M. E. Brown, D. A. Slayback, E. W. Pak, R. Mahoney, E. F. Vermote, and N. E. Saleous (2005), An extended AVHRR 8-km NDVI dataset compatible with MODIS and SPOT vegetation NDVI data, *Int. J. Remote Sens.*, *26*(20), 4,485–4,498.

Viste, E., and A. Sorteberg (2013). Moisture transport into the Ethiopian highlands, *Int. J. Climatol.*, *33*(1), 249–263.

Wang, K., and R. E. Dickinson (2012), A review of global terrestrial evapotranspiration: Observation, modeling, climatology, and climatic variability, *Rev. Geophys.*, *50*, RG2005, doi:10.1029/2011RG000373.

Wang, B., and Z. Fan (1999), Choice of South Asian summer monsoon indices, *Bull. Am. Meteorol. Soc.*, *80*(4), 629–638.

Wang, C., and Y. Guo (2011), Precipitable water conversion rates over the Qinghai-Xizang (Tibet) Plateau: Changing characteristics with global warming, *Hydrol. Processes*, *26*(10), 1,509–1,516.

Wang, B., Z. Wu, J. Li, J. Liu, C.-P. Chang, Y. Ding, and G. Wu (2008), How to measure the strength of the East Asian summer monsoon, *J. Climate*, *21*(17), 4,449–4,463.

Wang, X. M., C. X. Zhang, E. Hasi, and Z. B. Dong (2010), Has the Three Norths Forest Shelterbelt Program solved the desertification and dust storm problems in arid and semiarid China?, *J. Arid Environ.*, *74*(1), 13–22.

Wang, X., S. Piao, P. Ciais, J. Li, P. Friedlingstein, C. Koven, and A. Chen (2011), Spring temperature change and its implication in the change of vegetation growth in North America from 1982 to 2006, *Proc. Natl. Acad. Sci.*, *108*(4), 1,240–1,245.

Webster, P. J., and S. Yang (1992), Monsoon and ENSO: Selectively interactive systems, *Q. J. R. Meteorol. Soc.*, *118*(507), 877–926.

Wu, L. Y., J. Y. Zhang, and W. J. Dong (2011), Vegetation effects on mean daily maximum and minimum surface air temperatures over China, *Chin. Sci. Bull.*, *56*(9), 900–905.

Wu, Y. P., Y. P. Shen, and B. L. Li (2012), Possible physical mechanism of water vapor transport over Tarim River Basin, *Ecol. Complex.*, *9*, 63–70.

Xie, B., Q. Zhang, and Y. Ying (2011), Trends in precipitable water and relative humidity in China: 1979–2005, *J. Appl. Meteorol. and Climatol.*, *50*(10), 1,985–1,994.

Yan, H. S., J. Hu, K. Fan, and Y. J. Zhang (2007), The analysis of relationship between the variation of westerly index in summer and precipitation during the flood period over china in the last 50 Years, *Chin. J. Atmospheric Sci.*, *31*(4), 717–726.

Yang, X. C., Y. L. Zhang, M. J. Ding, L. S. Liu, Z. F. Wang, and D. W. Gao (2010), Observational evidence of the impact of vegetation cover on surface air temperature change in China, *Chinese J. Geophys.-Chinese Ed.*, *53*(4), 833–841.

Yu, P. T., V. Krysanova, Y. H. Wang, W. Xiong, F. Mo, Z. J. Shi, H. L. Liu, T. Vetter, and S. C. Huang (2009), Quantitative estimate of water yield reduction caused by forestation in a water-limited area in northwest China, *Geophys. Res. Lett.*, *36*, L02406, doi:10.1029/2008GL036744.

Zhai, P., and R. E. Eskridge (1997), Atmospheric water vapor over China, *J. Climate*, *10*(10), 2,643–2,652.

Zhang, Q., et al. (2007), Research on water-vapor distribution in the air over Qilian Mountains, *Acta Meteorol. Sin.*, *22*(1), 107–118.

Zhang, K., J. S. Kimball, R. R. Nemani, and S. W. Running (2010), A continuous satellite-derived global record of land surface evapotranspiration from 1983 to 2006, *Water Resour. Res.*, *46*(9), W09522, doi:10.1029/2009WR008800.

Zhang, J. Y., L. Y. Wu, G. Huang, W. Q. Zhu, and Y. Zhang (2011), The role of May vegetation greenness on the southeastern Tibetan Plateau for East Asian summer monsoon prediction, *J. Geophys. Res.-Atmos.*, *116*, D05106, doi:10.1029/2010JD015095.

Zheng, Y. Q., G. Yu, Y. F. Qian, M. Q. Miao, X. M. Zeng, and H. Q. Liu (2002), Simulations of regional climatic effects of vegetation change in China, *Q. J. R. Meteorol. Soc.*, *128*(584), 2,089–2,114.

Zheng, Y. Q., T. T. Long, X. M. Zeng, and X. M. Qiang (2011), Simulations of water resource changes in eastern and central China in the past 130 years by a regional climate model, *Acta Meteorol. Sin.*, *25*(5), 593–610.

Zou, X., P. Zhai, and Q. Zhang (2005), Variations in droughts over China: 1951–2003, *Geophys. Res. Lett.*, *32*, L04707, doi:10.1029/2004GL021853.